



PAPER

# Gamma radiation shielding properties of recycled polyvinyl chloride composites reinforced with micro/nano-structured PbO and CuO particles

To cite this article: Ahmed M El-Khatib *et al* 2021 *Phys. Scr.* **96** 125316

View the [article online](#) for updates and enhancements.

## You may also like

- [A Electrochemical Performance of Lead Oxide Nanostructure Prepared by Hydrometallurgical Leaching and Low-Temperature Calcination from Simulated Lead Paste](#)  
Linxia Gao, Jianwen Liu, Xinfeng Zhu et al.
- [Raman spectroscopy and X-ray diffraction studies on PbO and \(PbO\)<sub>1-x</sub>\(TiO<sub>2</sub>\)<sub>x</sub>](#)  
A Hedoux, D Le Bellac, Y Guinet et al.
- [Spray Pyrolyzed PbO-Carbon Nanocomposites as Anode for Lithium-Ion Batteries](#)  
S. H. Ng, J. Wang, K. Konstantinov et al.



## PAPER

# Gamma radiation shielding properties of recycled polyvinyl chloride composites reinforced with micro/nano-structured PbO and CuO particles

RECEIVED  
24 July 2021REVISED  
20 October 2021ACCEPTED FOR PUBLICATION  
2 November 2021PUBLISHED  
15 November 2021Ahmed M El-Khatib<sup>1</sup>, Yehia M Abbas<sup>2</sup>, Mohamed S Badawi<sup>3</sup>, Osama M Hagag<sup>4,\*</sup> and Mahmoud T Alabsy<sup>1</sup> <sup>1</sup> Physics Department, Faculty of Science, Alexandria University, 21511, Alexandria, Egypt<sup>2</sup> Department of Physics, Faculty of Science, Suez Canal University, Ismailia, Egypt<sup>3</sup> Department of Physics, Faculty of Science, Beirut Arab University, Beirut, Lebanon<sup>4</sup> Physics Department, Faculty of Science, Port Said University, Port Said, Egypt

\* Author to whom any correspondence should be addressed.

E-mail: [hagag82@yahoo.com](mailto:hagag82@yahoo.com)**Keywords:** recycled polyvinyl chloride, nano lead oxide, nano copper oxide, characterizations, linear attenuation coefficients, exposure buildup factors

## Abstract

In this work, the  $\gamma$ -ray shielding characteristics of fabricated recycled polyvinyl chloride (rPVC) loaded with micro and nano fillers of PbO and CuO composites were investigated. The PbO/rPVC and CuO/rPVC composites were prepared by changing the percentage of injected materials (PbO and CuO) between 10% and 40% with additions by 10%. Gamma-ray attenuation properties, such as mass attenuation coefficients, linear attenuation coefficients and half-value layer for PbO and CuO-supported polymers were obtained in the energy range between 59.5 and 1408.0 keV using narrow beam transmission geometry. These experiments were carried out by using a HPGe detector and five standard radioactive sources [<sup>241</sup>Am, <sup>133</sup>Ba, <sup>137</sup>Cs, <sup>60</sup>Co and <sup>152</sup>Eu]. Moreover, equivalent atomic numbers and the exposure buildup factor (EBF) values for incident photon energy in the range from 0.015 MeV to 15 MeV were also calculated by Geometric Progression (G-P) method. The experimental results revealed that, the measured values of the linear attenuation coefficients of the PbO/rPVC and CuO/rPVC composites showed their dependence on the type and the concentration of the filler (either PbO or CuO) and also on the incident gamma ray energy. Increasing the filler weight fractions wt.% in the rPVC matrix, increases the linear attenuation coefficients of the composite and the improvement is more significant in case of PbO compared to CuO of the same filler wt.% at the same energy. The results also demonstrated an enhancement in the radiation protection behavior of rPVC composites due to the addition of PbO and CuO fillers as nano-sized particles.

## 1. Introduction

The widespread use of ionizing radiation in various fields, including agriculture, industry, medicine, scientific research and other beneficial applications, has been increased in the last decades. Even though ionizing radiation has significant usages in many fields, it can cause harmful effects to workers when exposed to radiation doses higher than the permissible limit [1]. When the vital organs absorb these rays, it induces different types of reactions that will ionize the atoms inside the cell and then affect this balance and the normal functioning of these cells [2]. This damage may then manifest in the human body as medical symptoms such as radiation sickness, cataracts or, in the longer term, cancer [3]. Therefore, it is necessary to use effective shielding materials in radiological applications to attenuate different types of ionizing radiation and keep personnel protected against harmful effects of radiation.

Ionizing radiation, for example, gamma rays and x-rays, can be absorbed by elements with a large atomic number. Lead is the most widely used element in this field to protect from radiation due to its low cost and high

density. Using Lead in medical institutions for protection from ionizing radiation has some disadvantages since its mass is large, highly toxic, and dangerous to the environment [4]. Therefore, research on new materials which is less toxic and cost-effective besides preserving the environment is required to protect against radiation. Polymers are characterized by high chemical stability, high flexibility, low cost, and corrosion resistance [5]. Therefore, researchers are developing different polymer composites in many fields such as civil construction, automobiles, and mechanical engineering. Research on polymer composites as radiation protection materials has become an area of interest due to the ability to modify the composition of polymers as desired, where elements with large atomic number can be added to the polymer matrix to protect from radiation by photoelectric absorption, meanwhile, elements with low atomic number can be used as fillers to attenuate radiation by Compton scattering [6].

Different polymers such as natural rubber [4], high density polyethylene [7], ethylene-propylene-diene monomer (EPDM) [8], epoxy resin [9], polyester [10], polystyrene [11], and polyimide [12] were studied as radiation shielding matrixes against x-rays and  $\gamma$ -rays. Polyvinyl chloride (PVC) is a worldwide polymer which can be processed into a wide range of products. PVC is perhaps the most utilized thermoplastic material [13] in comparison with the overall polymer usages. This is due to its good mechanical characteristics, high performance, low cost, and corrosion resistance. It can also be used as an effective radiation shielding material due to its high density compared to other polymers. Mann *et al* compared the radiation shielding properties of six polymer and plastic materials experimentally in the energy range of 10–1400 keV. They demonstrated that PVC has the best attenuation for 10–110 keV gamma-rays [14]. In another research, PVC/tungsten micro composites were fabricated at different weight fractions of tungsten micro-particles and the shielding capability of the prepared samples were experimentally and theoretically tested against x-ray and  $\gamma$ -ray [15]. Additionally, A G Nunez-Brionesa *et al* prepared a gamma cross-linked PVC/ Bi<sub>2</sub>O<sub>3</sub> composites and demonstrated an improvement in the radiation shielding properties of the produced composites at different X-ray energies as a function of Bi<sub>2</sub>O<sub>3</sub> content [16]. Theoretical calculations of the shielding parameters of PVC, hematite/PVC and chalcocite/PVC composites were also reported between (0.015 < E < 15 MeV) using MCNP code [17].

In recent years, scientists have been attracted to the use of nanomaterials in various fields of science and technology. Continuous developments in the use of nanomaterials as fillers in the polymer matrix have been reported. Several researchers demonstrated the enhancement in the shielding capability of polymer composites by incorporating nanomaterials as fillers in the polymeric matrix. For example, El-Khatib *et al* studied the effect of particle size of CdO particles on  $\gamma$ -ray shielding characteristics of CdO/HDPE composites and concluded that CdO nanoparticles have a better gamma radiation shielding ability than micro-CdO particles [18]. Ran Li *et al* evaluated the mass attenuation coefficients of micro and nano Gd<sub>2</sub>O<sub>3</sub> reinforced epoxy composites and verified that nano- Gd<sub>2</sub>O<sub>3</sub> composites were more efficient to attenuate X and  $\gamma$ -rays than micro- Gd<sub>2</sub>O<sub>3</sub> composites [19]. The radiation shielding performance of Epoxy/Bi<sub>2</sub>O<sub>3</sub> and Epoxy/WO<sub>3</sub> micro and nano-structured composites have been also investigated [20]. This study revealed that the nano dopant is more effective in attenuating  $\gamma$ -rays than the micro dopant even if they are used in the same percentages. Another research reported that composites based on recycled high-density polyethylene as a matrix and filled PbO nanoparticles as fillers were the best shielding materials compared to those loaded with bulk PbO powder [21]. Asgari *et al* compared the radiation shielding features of micro and nano lead, bismuth and tungsten doped in elastomer composites against photon in wide energy range (40 keV to 662 keV). The results showed that better attenuation was achieved as the dimension of the particles was decreased to nano-size, especially at low photon energies [22].

The aim of this research is to develop sustainable, low-cost and effective radiation shielding composites based on recycled polyvinyl chloride filled with different weight fractions of PbO and CuO in the form of nano-sized and micro-sized particles. A comparative study is also performed to investigate the effect of particle size and the filler concentrations on the gamma-radiation shielding capability of PbO/rPVC versus CuO/rPVC composites. Field emission-transmission electron microscope (FE-TEM) is utilized to validate the size of the prepared nano PbO and nano CuO particles. The investigated rPVC composites were prepared by compression molding technique and also characterized by a scanning electron microscope (SEM). The linear attenuation coefficient and the half-value layer of the investigated composites are experimentally estimated at incident  $\gamma$ -ray energies ranging from 59.53 keV to 1408.01 keV by employing HPGe detector. Moreover, other shielding parameters, such as equivalent atomic number  $Z_{eq}$  and the exposure buildup factors (EBF) of the investigated rPVC composites are theoretically determined by employing the geometric progression method.

## 2. Materials and methods

### 2.1. Materials

Post-consumer recycled PVC from commercial sources (sewer pipes made primarily of polyvinyl chloride) were collected and cleaned by water to remove any undesirable debris, dried at 90 °C, crushed by a mechanical grinder

**Table 1.** The composite sample designations and the weight fraction % of filler in each composite.

Sample	rPVC (wt%)	Micro PbO (wt%)	Micro CuO (wt%)	Nano PbO (wt%)	Nano CuO (wt%)
Pure rPVC	100	—	—	—	—
10 wt% micro PbO	90	10	—	—	—
20 wt% micro PbO	80	20	—	—	—
30 wt% micro PbO	70	30	—	—	—
40 wt% micro PbO	60	40	—	—	—
10 wt% micro CuO	90	—	10	—	—
20 wt% micro CuO	80	—	20	—	—
30 wt% micro CuO	70	—	30	—	—
40 wt% micro CuO	60	—	40	—	—
10 wt% nano PbO	90	—	—	10	—
10 wt% nano CuO	90	—	—	—	10
5 wt% micro PbO + 5 wt% micro CuO	90	5	5	—	—
5 wt% nano PbO + 5 wt% nano CuO	80	—	—	5	5

and then shredded into small pellets and was used as a polymer matrix in this investigation. PbO and CuO in powder form were purchased from Loba Chemie Company and used as micro fillers.

## 2.2. Synthesis of CuO nano particles

CuO nanoparticles were chemically prepared [23] by adding 15 g ascorbic acid and 2 g CuSO<sub>4</sub> to 100 and 50 ml of hot water, respectively, and mixed for about 3 min and then left to dry for 12 h at 80 °C. Finally, the desiccated product was lightly ground by a pest of agate (The Mortar Grinder RM 200) and mortar to obtain a black precipitate.

## 2.3. Synthesis of PbO nano particles

PbO nanoparticles [24] was synthesized by adding 60 ml of 1 M lead acetate solution at 90 °C to a 50 ml of 19 M sodium hydroxide solution and then mixed until the appearance of orange red color. The obtained precipitate was separated and dried for 8 h at 100 °C. Finally, the desiccated product was lightly grounded by a pest of agate and mortar to obtain a yellow precipitate.

## 2.4. Fabrication of rPVC composites sheets

The investigated micro and nano rPVC composites were prepared by compression-molding technique [7]. Firstly, recycled PVC was molten in a two roll mixer at 190 °C for 15 min with a rotator speed set as 40 rpm and then mixed slowly with the filler powder with continuous blending for another 20 min to guarantee a homogenous mixed composite. The mixture was then poured into a stainless steel mold with dimensions of 40 × 40 cm<sup>2</sup> and thickness of 0.3 cm to be pressed using a hydraulic press with an applied pressure 10 MPa at 180 °C for 15 to produce a smooth homogeneous sample. Finally, every sample was cut into discs with diameter 8.4 cm by using a laser beam to study the gamma-ray attenuation properties. The composite sample designations and the weight fraction % of filler in each composite are listed in table 1.

## 2.5. Structural analysis

The particle size of PbO and CuO nanoparticles was analyzed by employing the field emission transmission electron microscope (FE-TEM) (JEM 1400 Plus, JEOL, Japan) at 200 kV. Moreover, a scanning electron microscope (SEM) (JSM-6010LV, JEOL) was also utilized to inspect the cross section morphologies of the fabricated rPVC composites. Before SEM observation, the specimens were coated with an ultrathin gold coating using a low-vacuum sputtering coating device (JEOL-JFC-1100E). The SEM micrographs were obtained at magnification order of 10,000x at 20 kV.

## 2.6. Gamma ray spectroscopy setup

The experimental gamma-ray measurements were obtained by using a  $\gamma$ -ray spectrometer which consists of (HPGe) hyper pure germanium crystal (25 × 25 × 0.3 cm<sup>3</sup>) with a multichannel analyzer and amplifier (MCA). The spectrometer is placed in a shield of 15 cm Pb layer with a liming layer of copper on the inner wall of the shield to reduce the background radiations and minimize the x-ray interference. The detector has relative efficiency of 15% in the energy range from 50 keV to 10 MeV and a resolution of 1.85 keV at 1.33 MeV gamma ray peak of <sup>60</sup>Co [25]. Gamma-radiation measurements in energy interval from 59.53 keV to 1408.01 keV obtained by using five standard radioactive point sources <sup>241</sup>Am, <sup>133</sup>Ba, <sup>137</sup>Cs, <sup>60</sup>Co, and <sup>152</sup>Eu. On 1 June 2009,

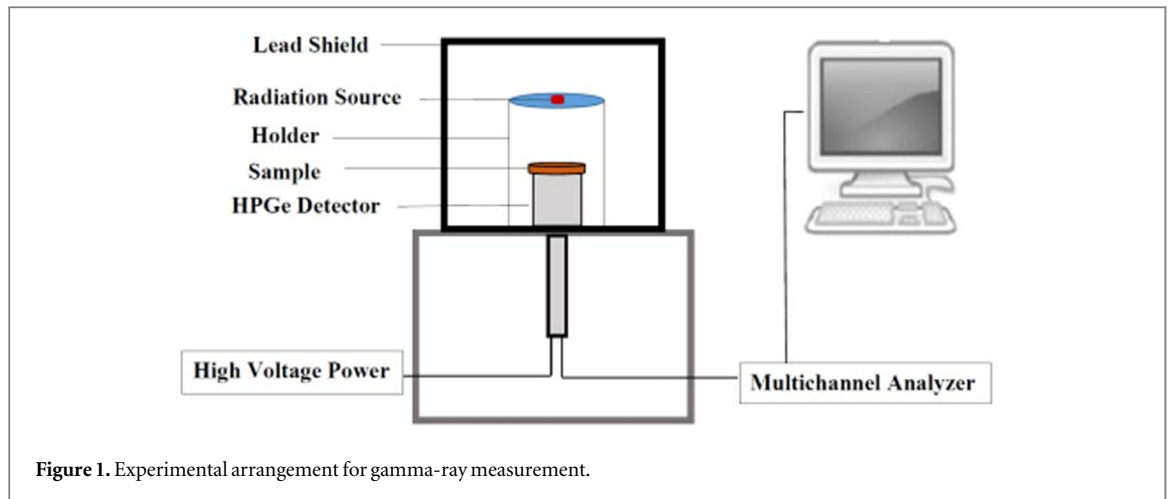


Figure 1. Experimental arrangement for gamma-ray measurement.

the initial activities of these sources were 259 kBq, 275.3 kBq, 385 kBq, 212.1 kBq, and 290 kBq, respectively. Currently, the present activities of these radioactive sources are 254.06 kBq, 125 kBq, 292.12 kBq, 43.78 kBq, and 156.85 kBq, respectively. During measurements, the radioactive source was placed at a height of 50.86 cm [26] to get a narrow beam and to minimize the errors due to the detector dead time.

The gamma spectra for all the measurements were collected enough times, according to the sample thickness, so that the statistical error would be less than 1%. Genie 2000 program was used to analyze the obtained spectra. The net area under each peak in the spectrum at given energy and thickness were tabulated in an excel sheet to calculate the shielding parameters of the prepared rPVC composites. The experimental arrangement for the gamma measurement system is displayed in figure 1.

## 2.7. Theoretical background

The linear attenuation coefficient ( $\mu$ ) of a material at an appropriate  $\gamma$ -ray energy can be determined from the well-known Beer–Lambert's law [18]:

$$\mu = \frac{1}{x} \ln \left( \frac{I_0}{I} \right) \quad (1)$$

where  $I_0$  and  $I$  are the incident and transmitted intensities, respectively, passing through a target material of thickness  $x$ . The mass attenuation coefficient ( $\mu/\rho$ ) can be calculated by dividing the estimated linear attenuation coefficient ( $\mu$ ) of a given sample by its density ( $\rho$ ) [27].

Half-value layer (HVL) is an essential parameter in choosing a suitable radiation shielding material and is defined as the absorber thicknesses needed to decrease the incident photon intensity to half of its initial value and is given by the following equation [28]:

$$HVL = \frac{\ln 2}{\mu} \quad (2)$$

The exposure buildup factor (EBF) is a significant parameter that must be taken into account in designing a shielding material. EBF is always greater than 1 and corrects the attenuation calculations in Lambert-Beer's law due to secondary emissions of gamma rays [29]. To calculate the EBF for the prepared rPVC composites, Geometric Progression (GP) fitting method was carried out according to the three following steps:

- (a) Equivalent atomic number ( $Z_{eq}$ ) of the composite, which is synonymous with the elemental atomic number, was first computed by the following equation [30]:

$$Z_{eq} = \frac{Z_1(\log R_2 - \log R) + Z_2(\log R - \log R_1)}{\log R_2 - \log R_1} \quad (3)$$

where  $R_1$  and  $R_2$  are the ( $\mu_{Comp}/\mu_{total}$ ) ratios corresponding to the elements with atomic numbers  $Z_1$  and  $Z_2$  respectively, and  $R$  is the ( $\mu_{Comp}/\mu_{total}$ ) ratio for the investigated composites at a specific energy, which lies between ratios  $R_1$  and  $R_2$ .

- (b) The obtained  $Z_{eq}$  values of the selected composites were then used to interpolate GP fitting exposure buildup factor coefficients (b, c, a,  $X_K$ , d) in the energy range 0.015-15 MeV using the interpolation formula [31] (4):

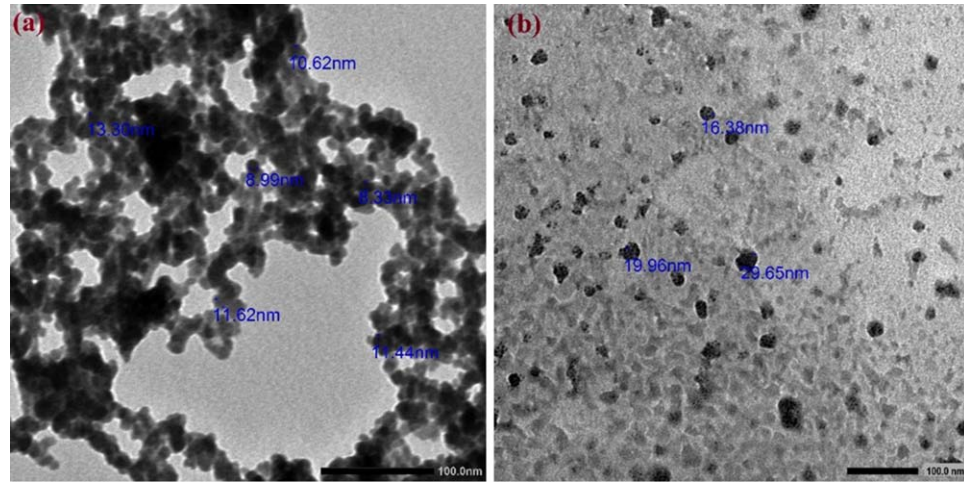


Figure 2. FE-TEM images of (a) PbO nanoparticles and (b) CuO nanoparticles.

$$C = \frac{C_1(\log Z_2 - \log Z_{eq}) + C_2(\log Z_{eq} - \log Z_1)}{\log Z_2 - \log Z_1} \quad (4)$$

where  $C_1$  and  $C_2$  are GP fitting parameters, taken from ANSI/ANS-6.4.3 standard database [32], corresponding to the atomic numbers  $Z_1$  and  $Z_2$  between which  $Z_{eq}$  of the prepared rPVC composite lies.

(c) Finally, the EBF were then computed with the help of the obtained GP fitting parameters, using the following relations [33]:

$$B(E, x) = 1 + \frac{b-1}{K-1} (K^x - 1), \quad K \neq 1 \quad (5)$$

and

$$B(E, x) = 1 + (b-1)x, \quad K = 1 \quad (6)$$

where

$$K(E, x) = cx^a + d \frac{\tanh(x/X_K - 2) - \tanh(-2)}{1 - \tanh(-2)} \quad \text{for } x \leq 40 \text{ mfp} \quad (7)$$

where  $E$  is incident photon energy and  $x$  is the penetration depth in terms of mfp.

## 3. Results and discussion

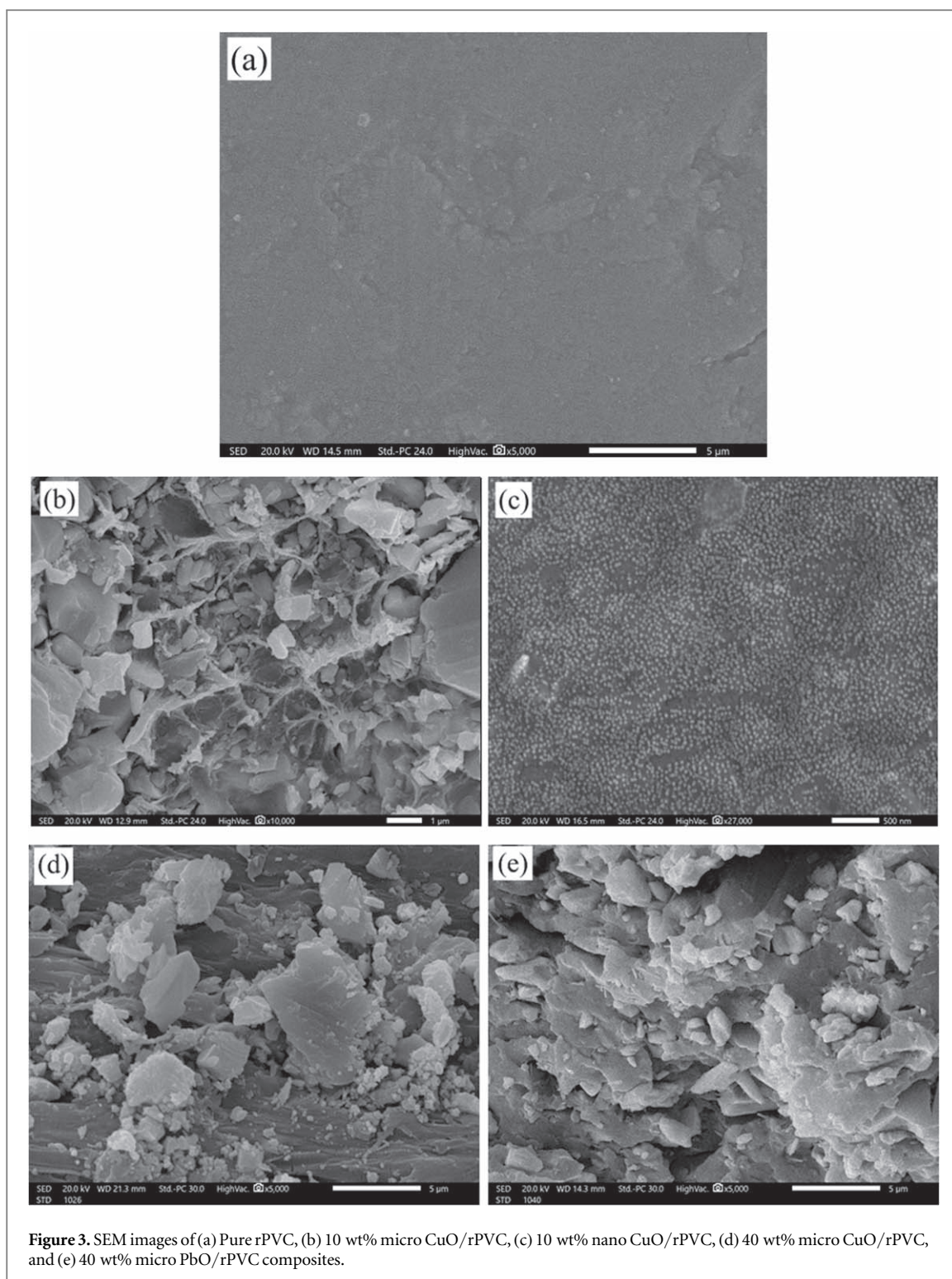
### 3.1. Characterization

#### 3.1.1. Field emission-transmission electron microscope (FE-TEM)

The FE-TEM micrographs of nano PbO and nano CuO particles are shown in figures 2(a) and (b) respectively. From figure 2(a), it is noticed that PbO nanoparticles have spherical shape with average particle size around 10 nm. In addition, figure 2(b) shows the presence of CuO nano particles with a uniform size distribution between 15 and 20 nm.

#### 3.1.2. Scanning electron microscope (SEM)

The SEM images of pure rPVC and rPVC composites loaded with 10 wt% micro CuO, 10 wt% nano CuO, 40 wt% micro CuO, and 40 wt% micro PbO are shown in figure 3. Figure 3 reveals that there is a clear variation between the morphology of pure rPVC (figure 3(a)) and CuO/rPVC composites (figures 3(b), (c)). It is also clear that, in the case of nanocomposites, CuO nanoparticles are scattered uniformly and well embedded in the rPVC matrix which provides an interlocking structure for shielding [34]. While, in the case of micro composites, bulky particles are not well covered with the rPVC matrix and some of them are peeled off from the matrix which acts as voids for shielding. Moreover, figures 3(d), (e) show typical SEM microphotographs of rPVC loaded with 40 wt% micro CuO and 40 wt% micro PbO, respectively. It can be observed that at higher filler loadings, both CuO and PbO micro particles of irregular shapes and different sizes are dispersed within the rPVC matrix where the gaps between the particles decreased compared to that in case of lower filler concentrations (figure 3(b)).



### 3.2. Gamma-ray shielding properties

#### 3.2.1. Mass and linear attenuation coefficients

The experimental linear attenuation coefficient  $\mu$  ( $\text{cm}^{-1}$ ) of the investigated rPVC composites can be evaluated at a given  $\gamma$ -ray energy according to the well-known Beer–Lambert formula given by  $\mu = \frac{1}{x} \ln \left[ \frac{N_{(0)}}{N_{(x)}} \right]$ , where  $N_{(0)}$  is the detector count rate without the sample and  $N_{(x)}$  is the count rate when the composite of thickness  $x$  is placed between the detector and the radioactive point source. To confirm the validity of our measurements, the mass attenuation coefficient  $\mu_m$  ( $\text{cm}^2/\text{g}$ ), which is a significant parameter for describing the interactions of gamma-rays with material, was calculated by dividing  $\mu$  by the density ( $\rho$ ) of the composite and compared with the theoretical  $\mu_m$  values obtained from the XCOM database [35]. The densities of the investigated composites

**Table 2.** Experimental and theoretical values of mass attenuation coefficients for micro and nano PbO/rPVC composites at different filler concentrations.

Sample	Energy (keV)	Mass attenuation coefficient (cm <sup>2</sup> /g)			Density (g/cm <sup>3</sup> )	
		Nano PbO/ rPVC	Micro PbO/ rPVC	XCOM	Nano PbO/ rPVC	Micro PbO/ rPVC
rPVC 0 wt%	59.53		0.5340	0.5106		1.646 ± 0.012
	80.99		0.2574	0.2494		
	121.78		0.3120	0.2920		
	244.69		0.1137	0.1089		
	344.22		0.0981	0.0943		
	356.01		0.0813	0.0760		
	661.66		0.0611	0.0596		
	778.90		0.0566	0.0541		
	964.13		0.0502	0.0481		
	1173.23		0.0467	0.0450		
1332.50		0.0377	0.0353			
1408.01		0.0320	0.0310			
10 wt% PbO	59.53	1.2031	1.1916	1.1643	1.870 ± 0.024	1.783 ± 0.018
	80.99	0.6026	0.5745	0.5406		
	121.78	0.7498	0.7044	0.6673		
	244.69	0.2132	0.2095	0.2045		
	344.22	0.1773	0.1711	0.1605		
	356.01	0.1511	0.1507	0.1413		
	661.66	0.1290	0.1100	0.1039		
	778.90	0.1142	0.1002	0.0941		
	964.13	0.1001	0.0949	0.0893		
	1173.23	0.0919	0.0862	0.0844		
1332.50	0.0821	0.0772	0.0726			
1408.01	0.0686	0.0658	0.0616			
20 wt% PbO	59.53		1.6676	1.6246		1.921 ± 0.033
	80.99		0.7404	0.6986		
	121.78		0.9494	0.9121		
	244.69		0.2832	0.2776		
	344.22		0.1835	0.1791		
	356.01		0.1645	0.1589		
	661.66		0.1198	0.1167		
	778.90		0.0954	0.0907		
	964.13		0.0905	0.0860		
	1173.23		0.0797	0.0745		
1332.50		0.0714	0.0670			
1408.01		0.0648	0.0611			
30 wt% PbO	59.53		1.7748	1.7464		2.140 ± 0.025
	80.99		0.8135	0.7717		
	121.78		1.1771	1.1451		
	244.69		0.3391	0.3338		
	344.22		0.2046	0.1985		
	356.01		0.1626	0.1574		
	661.66		0.1223	0.1201		
	778.90		0.0981	0.0959		
	964.13		0.0889	0.0865		
	1173.23		0.0754	0.0730		
1332.50		0.0666	0.0636			
1408.01		0.0621	0.0590			
40 wt% PbO	59.53		2.1072	2.0505		2.390 ± 0.021
	80.99		0.8647	0.8170		
	121.78		1.3957	1.3603		
	244.69		0.3452	0.3404		
	344.22		0.1945	0.1903		
	356.01		0.1775	0.1736		
	661.66		0.1171	0.1130		
	778.90		0.0924	0.0905		
	964.13		0.0856	0.0817		
	1173.23		0.0764	0.0730		
1332.50		0.0614	0.0580			
1408.01		0.0576	0.0542			

**Table 3.** Experimental and theoretical values of mass attenuation coefficients for micro and nano CuO/rPVC composites at different filler concentrations.

Sample	Energy (keV)	Mass attenuation coefficient ( $\text{cm}^2 \text{g}^{-1}$ )			Density ( $\text{g cm}^{-3}$ )	
		Nano CuO/rPVC	Micro CuO/rPVC	XCOM	Nano CuO/rPVC	Micro CuO/rPVC
10 wt% CuO	59.53	0.8726	0.8655	0.8547	$1.849 \pm 0.021$	$1.765 \pm 0.029$
	80.99	0.4885	0.4182	0.4051		
	121.78	0.5355	0.5274	0.5133		
	244.69	0.2077	0.1862	0.1790		
	344.22	0.1671	0.1559	0.1459		
	356.01	0.1415	0.1325	0.1278		
	661.66	0.1143	0.1004	0.0942		
	778.90	0.1000	0.0875	0.0834		
	964.13	0.0926	0.0830	0.0810		
	1173.23	0.0830	0.0747	0.0715		
20 wt% CuO	1332.50	0.0722	0.0627	0.0601	$1.895 \pm 0.019$	
	1408.01	0.0585	0.0505	0.0493		
	59.53		0.9112	0.8794		
	80.99		0.5882	0.5557		
	121.78		0.6725	0.6493		
	244.69		0.1835	0.1776		
	344.22		0.1665	0.1566		
	356.01		0.1391	0.1303		
	661.66		0.0986	0.0933		
	778.90		0.0862	0.0822		
30 wt% CuO	964.13		0.0836	0.0793	$2.054 \pm 0.024$	
	1173.23		0.0743	0.0714		
	1332.50		0.0649	0.0613		
	1408.01		0.0556	0.0527		
	59.53		0.9584	0.9289		
	80.99		0.5542	0.5377		
	121.78		0.7201	0.6907		
	244.69		0.1916	0.1832		
	344.22		0.1576	0.1491		
	356.01		0.1355	0.1295		
40 wt% CuO	661.66		0.1013	0.0954	$2.273 \pm 0.047$	
	778.90		0.0929	0.0881		
	964.13		0.0843	0.0817		
	1173.23		0.0726	0.0704		
	1332.50		0.0638	0.0602		
	1408.01		0.0580	0.0554		
	59.53		1.0169	0.9860		
	80.99		0.5239	0.5066		
	121.78		0.6639	0.6340		
	244.69		0.2426	0.2339		
344.22		0.1459	0.1381			
356.01		0.1344	0.1294			
661.66		0.1154	0.1104			
778.90		0.0890	0.0836			
964.13		0.0804	0.0772			
1173.23		0.0736	0.0702			
1332.50		0.0575	0.0552			
1408.01		0.0581	0.0549			

were measured experimentally by employing Archimedes procedure according to ASTM D 792-9124 [36], where, an electronic balance with accuracy 0.0001 g and organic liquid such as ethanol were used.

Tables 2–4 list out the measured densities, the experimental and the theoretical values of mass attenuation coefficients for micro and nano PbO/rPVC, CuO/rPVC and (PbO + CuO)/rPVC composites, respectively, at different gamma-ray energies. By examining tables 2–4, it can be noted that there is a good agreement between the experimental values of  $\mu_m$  for micro composites and the theoretical values obtained from XCOM which confirms the validity of our experimental setup. On the other hand, the values of  $\mu_m$  for all the rPVC nanocomposites are remarkably greater than those of micro composites even at the same wt.%. To study the

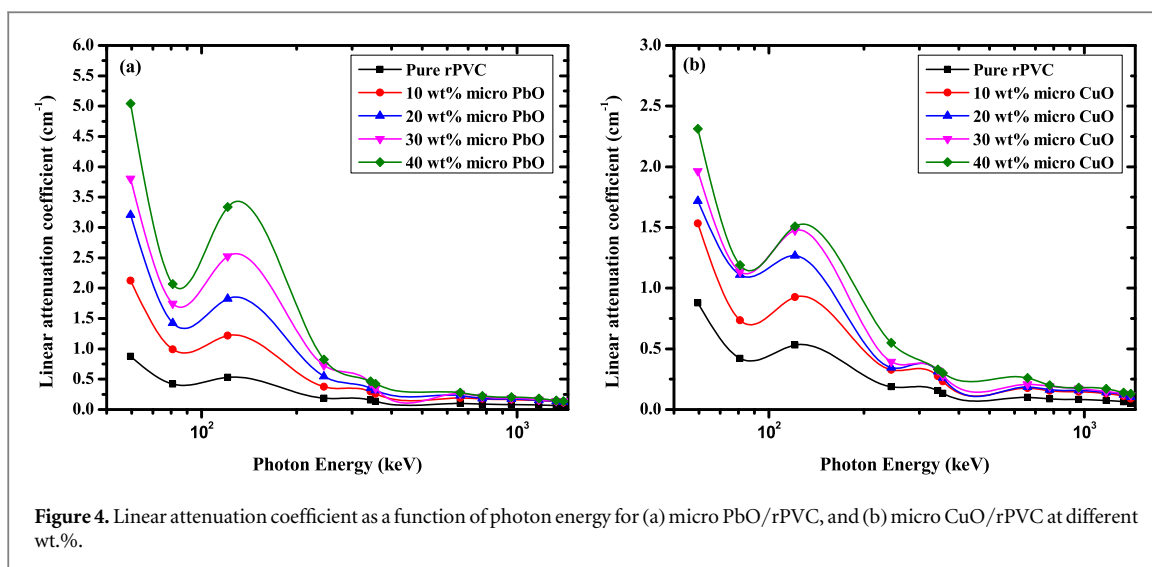


Figure 4. Linear attenuation coefficient as a function of photon energy for (a) micro PbO/rPVC, and (b) micro CuO/rPVC at different wt.%.

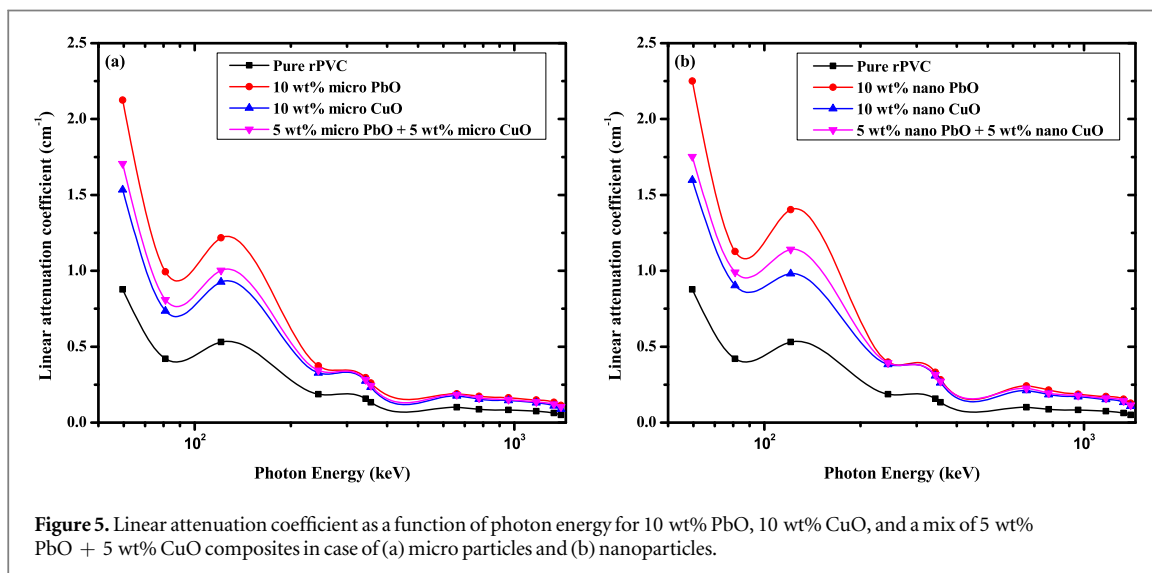


Figure 5. Linear attenuation coefficient as a function of photon energy for 10 wt% PbO, 10 wt% CuO, and a mix of 5 wt% PbO + 5 wt% CuO composites in case of (a) micro particles and (b) nanoparticles.

Table 4. Experimental and theoretical values of mass attenuation coefficients for micro and nano 5 wt% PbO + 5 wt% CuO/rPVC composites.

Sample	Energy (keV)	Mass attenuation coefficient (cm <sup>2</sup> g <sup>-1</sup> )			Density (g cm <sup>-3</sup> )	
		Nano mix/rPVC	Micro mix/rPVC	XCOM	Nano mix rPVC	Micro mix/rPVC
5 wt% PbO + 5 wt% CuO	59.53	0.9708	0.9660	0.9346	1.858 ± 0.032	1.766 ± 0.052
	80.99	0.5488	0.4578	0.4429		
	121.78	0.6316	0.5679	0.5495		
	244.69	0.2174	0.1948	0.1884		
	344.22	0.1744	0.1602	0.1550		
	356.01	0.1504	0.1377	0.1332		
	661.66	0.1248	0.1043	0.1010		
	778.90	0.1072	0.0918	0.0888		
	964.13	0.0992	0.0859	0.0831		
	1173.23	0.0895	0.0775	0.0750		
	1332.50	0.0797	0.0687	0.0664		
1408.01	0.0635	0.0588	0.0569			

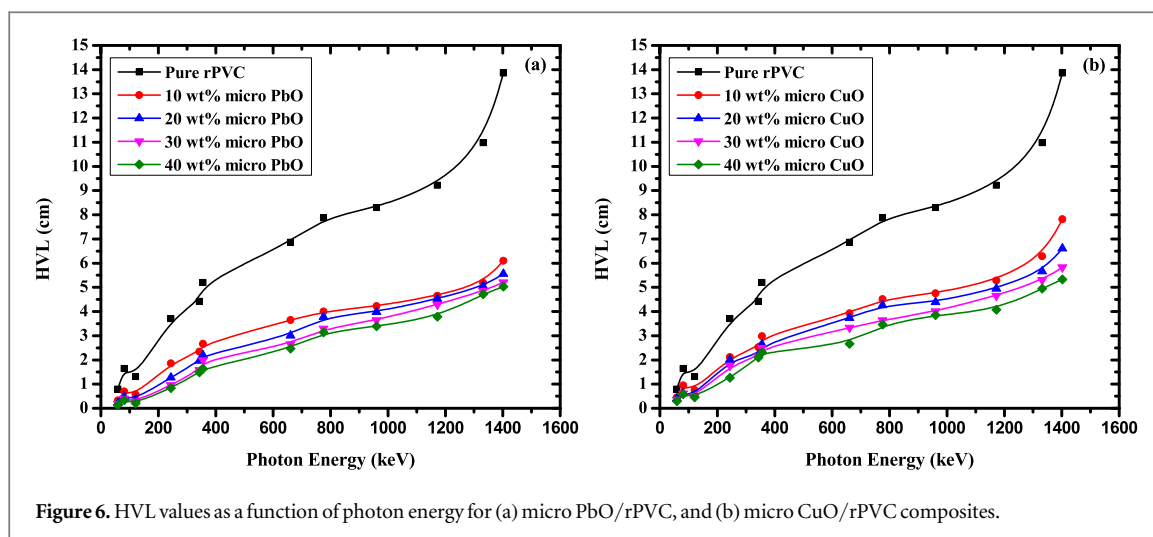


Figure 6. HVL values as a function of photon energy for (a) micro PbO/rPVC, and (b) micro CuO/rPVC composites.

effect of adding PbO and CuO fillers on the shielding ability of the rPVC matrix, it is better to compare between them in terms of linear attenuation coefficients.

Figures 4(a) and (b) depict the variation of linear attenuation coefficients of micro PbO/rPVC and micro CuO/rPVC composites, respectively, as a function of gamma-ray energy at different filler concentrations. As a first estimate from inspecting figure 4, one can find that the shielding properties depend on the chemical composition of the shielding material and the energy of the falling  $\gamma$ -beams. This is evident from figures 4(a) and (b) where the linear attenuation coefficient decreases sharply by increasing the incident photon energy and increases significantly by increasing the concentrations of PbO and CuO fillers in the rPVC matrix. This conduct can be ascribed due to the predominance of various photon interactions with matter which are photoelectric effect, Compton scattering, and pair production by which the gamma-ray dissipates its energy. For energy less than 200 keV the most probable interactions of photons are photoelectric effect, but for photons greater than 200 keV this probability will drop with energy and the dominant interactions will be the Compton effect [37]. It is also remarked from figure 4 that,  $\mu$  of all the composites have a peak value at energy 121.78 keV and this peak is very sharp specially in PbO/rPVC composites. This peak is due to appearance of the K absorption edge of Pb at 88 keV [38]. The peak is also appeared in neat rPVC and CuO/rPVC composites because the recycled PVC contains a small amount of Pb.

Furthermore, figure 5(a) compares the linear attenuation coefficients of 10 wt.% micro PbO/rPVC, 10 wt.% micro CuO/rPVC and (5 wt.% micro PbO + 5 wt.% micro CuO)/rPVC composites. It is observed that,  $\mu$  values of PbO/rPVC composites are greater than those for CuO/rPVC composites of the same filler concentration at lower energies. This is owing to the high gamma-ray absorption of Pb compared to Cu in this energy region. However, at energies higher than 300 keV, CuO/rPVC composite has approximately the same linear attenuation coefficient as PbO/rPVC of the same wt%. The  $\mu$  values for the mixture of both PbO and CuO is between those of PbO/rPVC composites and CuO/rPVC composites in any energy region as indicated by figure 5(a).

In order to understand the significance role of adding nano additives to the rPVC matrix, the linear attenuation coefficients as a function of photon energy for 10 wt.% nano PbO/rPVC, 10 wt.% nano CuO/rPVC and (5 wt.% nano PbO + 5 wt.% nano CuO)/rPVC composites are depicted in figure 5(b). It is clear that, the same behavior of  $\mu$  versus photon energy is obtained as in figure 5(a). Moreover, figure 5(b) and tables 2–4 also demonstrated that, the rPVC composites reinforced with nano-fillers of PbO or CuO have higher linear attenuation coefficients compared to those filled with micro-fillers of the same weight fraction, which is consistent with the results reported in the literature [21]. This is due to the homogenous distribution of nano-fillers within the rPVC matrix, as confirmed by the SEM micrographs, which enhances the probability of interaction between gamma-rays and nanoparticles.

To assess the  $\gamma$ -ray shielding performances of the composites presented in this work, the linear attenuation coefficient of 40 wt% micro PbO/rPVC composite is compared to various polymer composites reported in references as listed in table 5. From table 5, it is evident that 40 wt% micro PbO/rPVC exhibits higher shielding ability than the other polymer composites even at the same filler concentration, while lower ability than high concentration of PbO filled polymer composites. Therefore, PbO filled rPVC composite is a promising protective material against gamma-radiation.

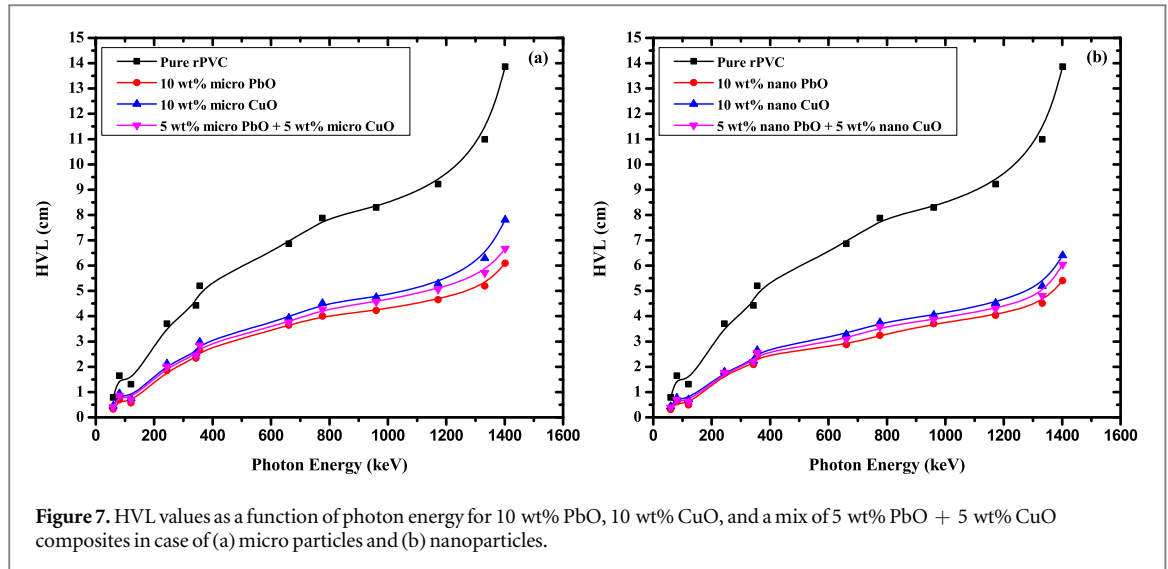


Figure 7. HVL values as a function of photon energy for 10 wt% PbO, 10 wt% CuO, and a mix of 5 wt% PbO + 5 wt% CuO composites in case of (a) micro particles and (b) nanoparticles.

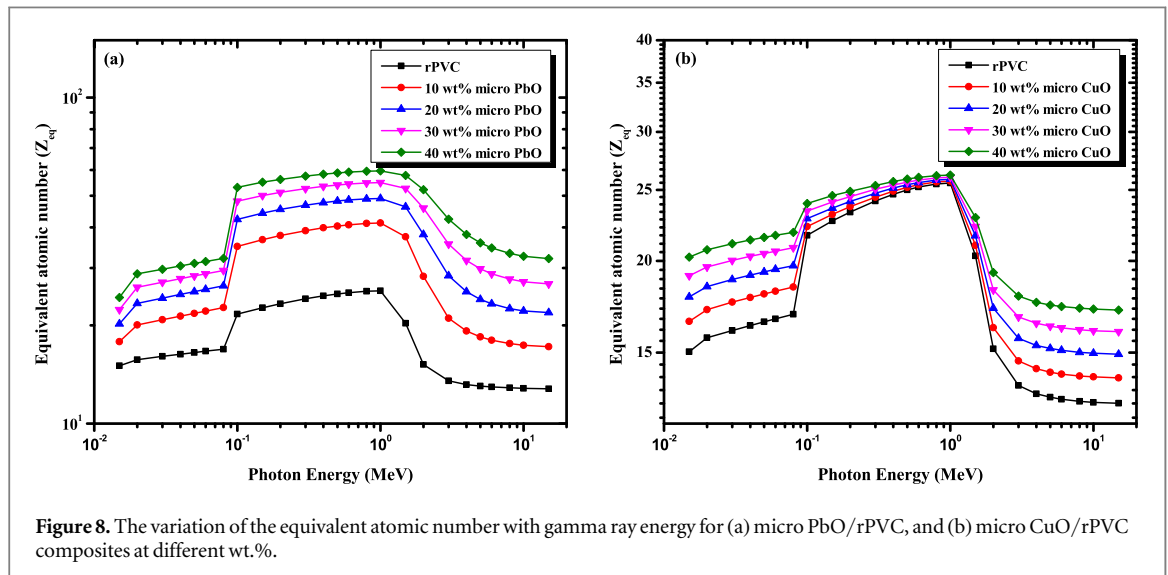


Figure 8. The variation of the equivalent atomic number with gamma ray energy for (a) micro PbO/rPVC, and (b) micro CuO/rPVC composites at different wt.%.

Table 5. Reported shielding performances of polymer-based composites in references at similar photon energies.

Shielding material	Linear attenuation coefficient (cm <sup>-1</sup> )			References
	59.53 keV	661.66 keV	1332.5 keV	
40 wt% nano ZnO/HDPE	0.946	0.121	0.086	[1]
40 wt% nano CdO/HDPE	4.030	0.147	0.100	[18]
50 wt% nano PbO/rHDPE	5.760	0.241	0.134	[21]
50 wt.% hematite/PES	1.170	0.190	0.150	[39]
20 wt% BiClO /polyester concretes	1.182	0.121	0.080	[40]
100 phr PbO/WR/NR	—	0.187	0.126	[41]
40 wt% micro PbO/rPVC	5.041	0.280	0.147	This work

Note: HDPE is high density polyethylene; PES is isophthalic unsaturated polyester; WR is waste rubber; NR natural rubber; phr is Part per hundred parts of rubber by weight.

### 3.2.2. Half value layer

The halve value layer (HVL) is one of the essential shielding parameters which evaluate the thickness of the shielding material required to diminish the radiation intensity to 50% of its initial value. Figures 6(a) and (b) display the computed HVL values of micro PbO/rPVC and micro CuO/rPVC composites, respectively, at the

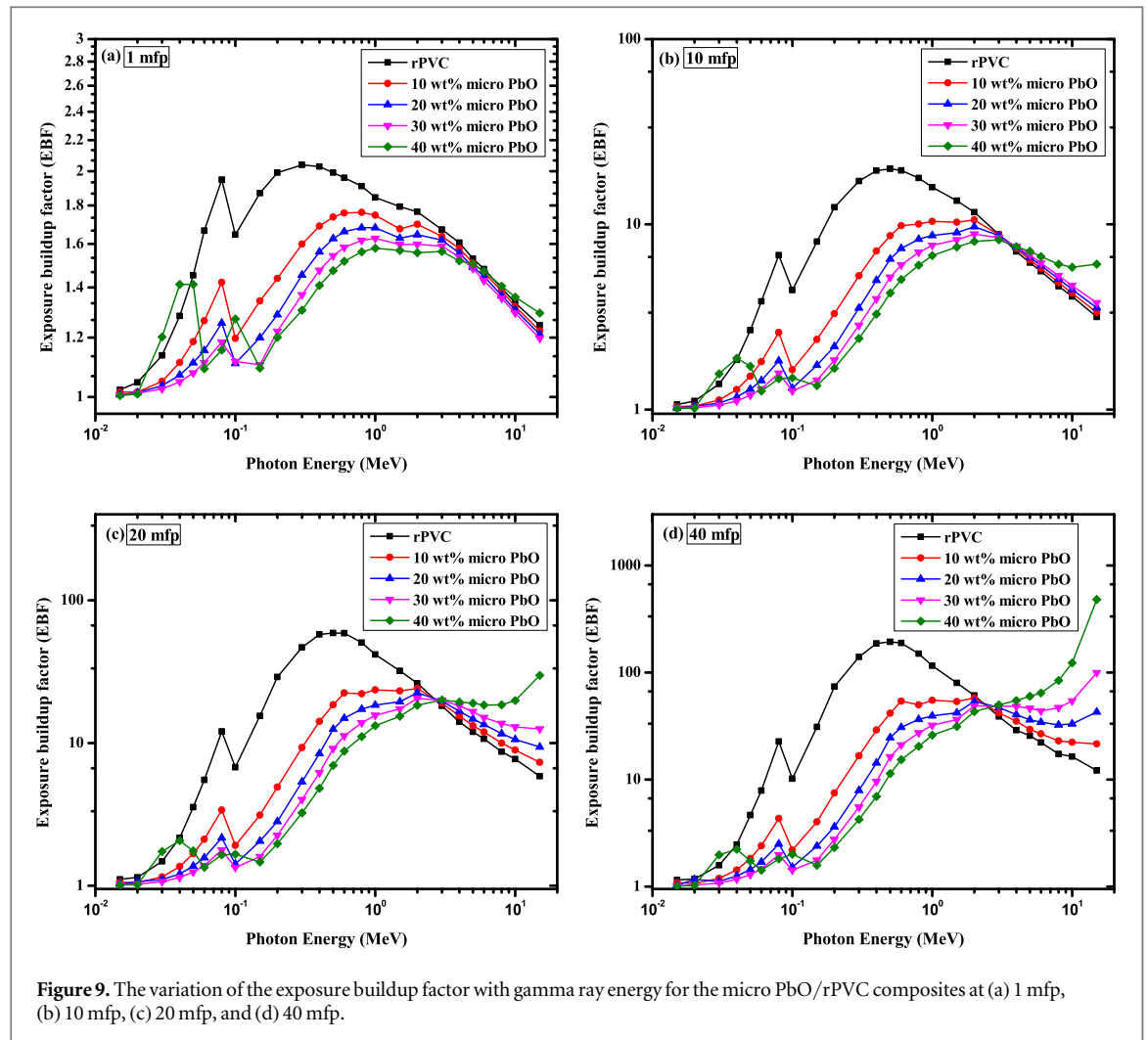


**Figure 9.** The variation of the exposure buildup factor with gamma ray energy for the micro PbO/rPVC composites at (a) 1 mf, (b) 10 mf, (c) 20 mf, and (d) 40 mf.

same variation of the filler concentration to assess their shielding ability. From figure 6 it is clear that, for all the investigated composites, as the energy increases the HVL values will also increase. It is also obvious from the figure 6 that the HVL values of the rPVC composites are much lower than that of pure rPVC at any given energy which indicates an enhancement in the shielding properties of the rPVC composites by adding PbO and CuO fillers.

Moreover, figure 7(a) compares the HVL values of 10 wt.% micro PbO/rPVC, 10 wt.% micro CuO/rPVC and (5 wt.% micro PbO + 5 wt.% micro CuO)/rPVC composites. It can be noted that, the HVL value of CuO/rPVC composites is greater than its corresponding value for PbO/rPVC composites at the same weight percent and that regarding the mixture of both PbO and CuO is always between those of PbO/rPVC composites and CuO/rPVC composites in any energy region. Figure 7(b) presents the HVL values as a function of photon energy for 10 wt.% nano PbO/rPVC, 10 wt.% nano CuO/rPVC and (5 wt.% nano PbO + 5 wt.% nano CuO)/rPVC composites. It is evident that, same behavior and trends are achieved as in figure 6(a), however, nanocomposites always have lower HVL values than micro composites at any incident photon energy. This results in higher shielding performance of nanocomposites, which is consistent with the former analysis.

### 3.2.3. Equivalent atomic number

The perfect protective composite is that which have the higher equivalent atomic number [27]. Figure 8 displays the variation of  $Z_{eq}$  values against gamma-ray energy of micro PbO/rPVC and micro CuO/rPVC, composites at different wt.%. Figure 8 reveals that  $Z_{eq}$  values of all composites depend on the incident photon energy. Moreover, it is clear from figure 8 that increasing the weight fractions of PbO or CuO fillers to the rPVC leads to an increase in the  $Z_{eq}$  values of the composites. The highest  $Z_{eq}$  value is obtained for 40 wt% PbO/rPVC composite and the pure rPVC without any filler addition has the smallest  $Z_{eq}$  values. For this reason, 40 wt.% micro PbO/rPVC composite has the highest attenuation coefficient compared with that loaded by micro CuO at the same wt.%, which is consistent with the former results.

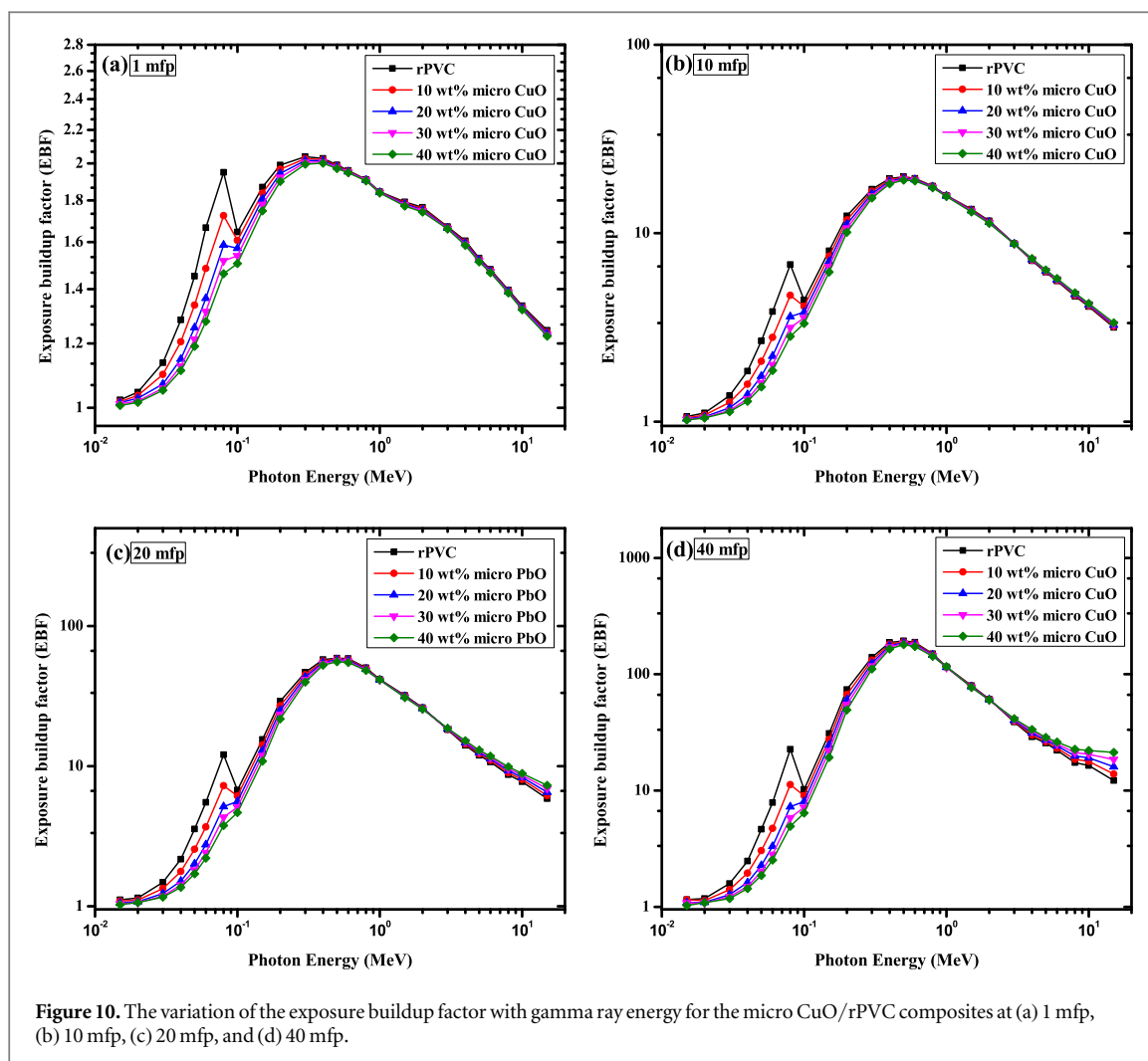


**Figure 10.** The variation of the exposure buildup factor with gamma ray energy for the micro CuO/rPVC composites at (a) 1 mfp, (b) 10 mfp, (c) 20 mfp, and (d) 40 mfp.

### 3.2.4. Exposure buildup factor

The variation of the EBF with a photon energy between 0.015 and 15 MeV of the PVC composites filled with different wt.% of PbO and CuO are displayed in figures 9 and 10 respectively at penetration depths 1, 10, 20, and 40 mfp. It is clear from figures 9–10 that, the EBF for all PVC composites are small in low energy region and slightly increase by increasing the penetration depth up to 40 mfp. These small EBF values could be attributed to the photoelectric effects, where all photons are completely removed from the material at low photon energies [29]. In other words, the increase in penetration depth leads to an increase in the interaction of photons with the sample, which leads to the generation of a large number of low-energy photons. It is also obvious that there is a peak in the EBF that occurs at 80 keV in all the investigated composites corresponding to K-edge absorption of Pb (i.e. 88 keV) and this peak is very sharp in PbO/rPVC composites compared with CuO/rPVC composites (figure 10). This peak has also appeared in the CuO composites because the base rPVC itself contains a small amount of Pb.

Furthermore, the maximum EBF for is obtained in the intermediate energy where the EBF value appears to be very large which is considered as a general trend for all the investigated rPVC composites. This is due to the Compton scattering process, where the photon is not completely removed, but its energy is reduced through multiple scattering, which raises the EBF to a maximum value between 0.1 and 1 MeV. Additionally, increasing the filler weight fraction in the rPVC matrix decreases the EBF. This is attributed to the increase in attenuation probability of photons due to the increase in the concentrations of Pb and Cu elements which is consistent with the former results. It is also noticed that at 3 MeV all the composites have nearly the same value of EBF and after 3 MeV the trend is reversed where increasing the filler weight fraction would increase the EBF values. This trend is especially observed at 20 and 40 mfp for PbO/rPVC composites as shown in figure 9. The trend of EBF between 3 and 15 MeV is due to pair production, which is the most important process at these high energies. Moreover, in the case of CuO/rPVC composites shown in figure 10, it is obvious that increasing the percentage of CuO filler does not have a significant effect on the EBF at the same photon energy.

## 4. Conclusion

In this paper, sustainable and low-cost composites based on rPVC, filled with different weight fractions of PbO and CuO in the form of nano-sized and micro-sized particles, were investigated as protective gamma-radiation shielding composites. From the obtained results, it can be concluded that:

- There is a good agreement between the experimental values of the mass attenuation coefficients for micro composites and those obtained theoretically from the XCOM database.
- The measured values of the linear attenuation coefficients showed their dependence on the type and the concentration of the filler (either PbO or CuO) and also on the incident gamma ray energy.
- Increasing the filler weight fractions wt.% in the rPVC matrix, increases the linear attenuation coefficients of the composite and the improvement is more significant in case of PbO compared to CuO of the same filler wt.% at the same energy.
- The rPVC composites reinforced with nano-fillers of PbO or CuO have better gamma-radiation shielding capability compared to those filled with micro-fillers of the same weight fraction.
- The values of the equivalent atomic number and the exposure buildup factors of the investigated composites depend on the incident photon energy and the concentration of the filler in the composites.
- PbO/rPVC and CuO/rPVC composites can be suggested as good candidates for  $\gamma$ -ray protecting requests, for example in radiation research centers, oncology departments in hospitals, and in radiological applications.

## Data availability statement

All data that support the findings of this study are included within the article (and any supplementary files).

## ORCID iDs

Mahmoud T Alabsy  <https://orcid.org/0000-0002-6333-5102>

## References

- [1] Alsayed Z, Badawi M S, Awad R, Elkhatib A and Thabet A 2020 Investigation of  $\gamma$ -ray attenuation coefficients, effective atomic number and electron density for ZnO/HDPE composite *Phys. Scr.* **95** 085301
- [2] Elgazzar A H and Kazem N 2015 Biological effects of ionizing radiation *The Pathophysiologic Basis of Nuclear Medicine* (Berlin: Springer) pp 715–26
- [3] Martin A, Harbison S, Beach K and Cole P 2018 *An Introduction to Radiation Protection* (Boca Raton, FL: CRC Press)
- [4] Kalkornsuraprane E, Kothan S, Intom S, Johns J, Kaewjaeng S, Kedkaew C, Chaiphaksa W, Sareein T and Kaewkhao J 2021 Wearable and flexible radiation shielding natural rubber composites: effect of different radiation shielding fillers *Radiat. Phys. Chem.* **179** 109261
- [5] More C V, Alsayed Z, Badawi M S, Thabet A A and Pawar P P 2021 Polymeric composite materials for radiation shielding: a review *Environ. Chem. Lett.* **19** 2057–90
- [6] Tekin H O, Kaçal M R, Issa S A M, Polat H, Susoy G, Akman F, Kilicoglu O and Gillette V H 2020 Sodium dodecatungstophosphate hydrate-filled polymer composites for nuclear radiation shielding *Mater. Chem. Phys.* **256** 123667
- [7] Alharshan G A, Aloraini D A, Elzaher M A, Badawi M S, Alabsy M T, Abbas M I and El-Khatib A M 2020 A comparative study between nano-cadmium oxide and lead oxide reinforced in high density polyethylene as gamma rays shielding composites *Nucl. Technol. Radiat. Prot.* **35** 42–9
- [8] Poltabtim W, Wimolmala E and Saenboonruang K 2018 Properties of lead-free gamma-ray shielding materials from metal oxide/EPDM rubber composites *Radiat. Phys. Chem.* **153** 1–9
- [9] Higgins M C M, Radcliffe N A, Toro-González M and Rojas J V 2019 Gamma ray attenuation of hafnium dioxide-and tungsten trioxide-epoxy resin composites *J. Radioanal. Nucl. Chem.* **322** 707–16
- [10] Kaçal M R, Polat H, Oltulu M, Akman F, Agar O and Tekin H O 2020 Gamma shielding and compressive strength analyses of polyester composites reinforced with zinc: an experiment, theoretical, and simulation based study *Appl. Phys. A* **126** 1–15
- [11] Pavlenko V I, Lipkanskii V M and Yastrebinskii P N 2004 Calculations of the passage of gamma-quanta through a polymer radiation-protective composite *J. Eng. Phys. Thermophys.* **77** 11–4
- [12] Wang P, Tang X, Chai H, Chen D and Qiu Y 2015 Design, fabrication, and properties of a continuous carbon-fiber reinforced  $\text{Sm}_2\text{O}_3$ /polyimide gamma ray/neutron shielding material *Fusion Eng. Des.* **101** 218–25
- [13] Sadat-Shojai M and Bakhshandeh G-R 2011 Recycling of PVC wastes *Polym. Degrad. Stab.* **96** 404–15
- [14] Mann K S, Rani A and Heer M S 2015 Shielding behaviors of some polymer and plastic materials for gamma-rays *Radiat. Phys. Chem.* **106** 247–54
- [15] Abdolazadeh T, Morshedian J, Ahmadi S, Ay M R and Mohammadi O 2021 Introducing a novel polyvinyl chloride/tungsten composites for shielding against gamma and x-ray radiations *Iran. J. Nucl. Med.* **29** 58–64

- [16] Nuñez-Briones A G, Benavides R, Mendoza-Mendoza E, Martínez-Pardo M E, Carrasco-Abrego H, Kotzian C, Saucedo-Zendejo F R and Garcia-Cerda L A 2021 Preparation of PVC/Bi<sub>2</sub>O<sub>3</sub> composites and their evaluation as low energy x-ray radiation shielding *Radiat. Phys. Chem.* **179** 109198
- [17] Mahmoud K A, Lacomme E, Sayyed M I, Özpolat Ö F and Tashlykov O L 2020 Investigation of the gamma ray shielding properties for polyvinyl chloride reinforced with chalcocite and hematite minerals *Heliyon* **6** e03560
- [18] El-Khatib A M, Abbas M I, Elzاهر M A, Badawi M S, Alabsy M T, Alharshan G A and Aloraini D A 2019 Gamma attenuation coefficients of nano cadmium oxide/high density polyethylene composites *Sci. Rep.* **9** 16012
- [19] Li R, Gu Y, Wang Y, Yang Z, Li M and Zhang Z 2017 Effect of particle size on gamma radiation shielding property of gadolinium oxide dispersed epoxy resin matrix composite *Mater. Res. Express* **4** 35035
- [20] Karabul Y and İçelli O 2021 The assessment of usage of epoxy based micro and nano-structured composites enriched with Bi<sub>2</sub>O<sub>3</sub> and WO<sub>3</sub> particles for radiation shielding *Results Phys.* **26** 104423
- [21] Mahmoud M E, El-Khatib A M, Badawi M S, Rashad A R, El-Sharkawy R M and Thabet A A 2018 Recycled high-density polyethylene plastics added with lead oxide nanoparticles as sustainable radiation shielding materials *J. Clean. Prod.* **176** 276–87
- [22] Asgari M, Afarideh H, Ghafoorifard H and Amirabadi E A 2021 Comparison of nano/micro lead, bismuth and tungsten on the gamma shielding properties of the flexible composites against photon in wide energy range (40 keV to 662 keV) *Nucl. Eng. Technol.* **53** 4142–9
- [23] Liu Q, Yasunami T, Kuruda K and Okido M 2012 Preparation of Cu nanoparticles with ascorbic acid by aqueous solution reduction method *Trans. Nonferrous Met. Soc. China* **22** 2198–203
- [24] Alagar M, Theivasanthi T and Raja A K 2012 Chemical synthesis of nano-sized particles of lead oxide and their characterization studies arXiv1204.0896
- [25] EL-Khatib A M, Gouda M M, Badawi M S, Nafee S and EL-Mallah E A 2013 Computation of the full energy peak efficiency of an HPGE detector using a new compact simulation analytical approach for spherical sources *J. Eng. Sci. Technol.* **8** 623–38
- [26] El-Khatib A M, Salem B A, Badawi M S, Gouda M M, Thabet A A and Abbas M I 2017 Full-Energy peak efficiency of an NaI (Tl) detector with coincidence summing correction showing the effect of the source-to-detector distance *Chinese J. Phys.* **55** 478–89
- [27] Mahmoud K A, Sayyed M I and Tashlykov O L 2019 Gamma ray shielding characteristics and exposure buildup factor for some natural rocks using MCNP-5 code *Nucl. Eng. Technol.* **51** 1835–41
- [28] Kiani M A, Ahmadi S J, Outokesh M, Adeli R and Kiani H 2019 Study on physico-mechanical and gamma-ray shielding characteristics of new ternary nanocomposites *Appl. Radiat. Isot.* **143** 141–8
- [29] Akyildirim H, Kavaz E, El-Agawany F I, Yousef E and Rammah Y S 2020 Radiation shielding features of zirconolite silicate glasses using XCOM and FLUKA simulation code *J. Non. Cryst. Solids* **545** 120245
- [30] Harima Y 1983 An approximation of gamma-ray buildup factors by modified geometrical progression *Nucl. Sci. Eng.* **83** 299–309
- [31] Sharaf J M and Saleh H 2015 Gamma-ray energy buildup factor calculations and shielding effects of some Jordanian building structures *Radiat. Phys. Chem.* **110** 87–95
- [32] American Nuclear Society 1991 *Gamma-Ray Attenuation Coefficients and Buildup Factors for Engineering Materials* **138**
- [33] Harima Y, Sakamoto Y, Tanaka S and Kawai M 1986 Validity of the geometric-progression formula in approximating gamma-ray buildup factors *Nucl. Sci. Eng.* **94** 24–35
- [34] El-Khatib A M, Hamada M S, Alabsy M T, Youssef Y M, Elzاهر M A, Badawi M S, Fayez-Hassan M, Kopatch Y N, Ruskov I N and Abbas M I 2021 Fast and thermal neutrons attenuation through micro-sized and nano-sized CdO reinforced HDPE composites *Radiat. Phys. Chem.* **180** 109245
- [35] Berger M J, Hubbell J H, Seltzer S M, Chang J, Coursey J S, Sukumar R, Zucker D S and Olsen K 2010 XCOM: Photon cross sections database, 2010 URL <http://nist.gov/pml/data/xcom>
- [36] ASTM 1997 Standard test methods for density and specific gravity (Relative Density) of plastics by displacement (D 792-91)
- [37] Biswas R, Sahadath H, Mollah A S and Huq M F 2016 Calculation of gamma-ray attenuation parameters for locally developed shielding material: polyboron *J. Radiat. Res. Appl. Sci.* **9** 26–34
- [38] McCaffrey J P, Shen H, Downton B and Mainegra-Hing E 2007 Radiation attenuation by lead and nonlead materials used in radiation shielding garments *Med. Phys.* **34** 530–7
- [39] Belgin E E, Aycik G A, Kalemtaş A, Pelit A, Dilek D A and Kavak M T 2015 Preparation and characterization of a novel ionizing electromagnetic radiation shielding material: hematite filled polyester based composites *Radiat. Phys. Chem.* **115** 43–8
- [40] Sharma A, Sayyed M I, Agar O, Kaçal M R, Polat H and Akman F 2020 Photon-shielding performance of bismuth oxychloride-filled polyester concretes *Mater. Chem. Phys.* **241** 122330
- [41] El-Khatib A M, Doma A S, Badawi M S, Abu-Rayyan A E, Aly N S, Alzahrani J S and Abbas M I 2020 Conductive natural and waste rubbers composites-loaded with lead powder as environmental flexible gamma radiation shielding material *Mater. Res. Express* **7** 105309